

# Stretch Activation and Nonlinear Elasticity of Muscle Cross-Bridges

N. Thomas\* and R. A. Thornhill†

\*School of Physics and Space Research and †School of Biological Sciences, The University of Birmingham, Birmingham B15 2TT England

**ABSTRACT** When active insect fibrillar flight muscle is stretched, its ATPase rate increases and it develops “negative viscosity,” which allows it to perform oscillatory work. We use a six-state model for the cross-bridge cycle to show that such “stretch activation” may arise naturally as a nonlinear property of a cross-bridge interacting with a single attachment site on a thin filament. Attachment is treated as a thermally activated process in which elastic energy must be supplied to stretch or compress the cross-bridge spring. We find that stretch activation occurs at filament displacements where, before the power stroke, the spring is initially in compression rather than in tension. In that case, pulling the filaments relieves the initial compression and reduces the elastic energy required for attachment. The result is that the attachment rate is enhanced by stretching. The model also displays the “delayed tension” effect observed in length-step experiments. When the muscle is stretched suddenly, the power stroke responds very quickly, but there is a time lag before dissociation at the end of the cycle catches up with the increased attachment rate. This lag is responsible for the delayed tension and hence also for the negative viscosity.

## INTRODUCTION

From a physical point of view, muscle is a nonlinear mechanical system. A striking example of this nonlinearity is found in fibrillar insect flight muscle, which has the remarkable property that it produces self-sustained oscillations of an insect's wings in response to asynchronous nervous impulses (Pringle, 1949). Machin and Pringle (1959) showed that the flight muscle has a negative loss, or “negative viscosity,” at the wing beat frequency, and that this sustains the oscillations by coupling to the mechanical resonator formed by the insect's wings and thorax. However, even in the presence of the essential ingredients of calcium and ATP, the resting stiffness of insect flight muscle at zero tension is very low (White et al., 1977). The muscle becomes much stiffer and develops negative viscosity only when it is held under a bias tension, demonstrating that its elastic properties are indeed decidedly nonlinear. Furthermore, one finds that the rate of ATP hydrolysis by the flight muscle also increases in response to the bias tension (Rüegg and Tregear, 1966; Rüegg and Stumpf, 1969). This phenomenon and the ability to perform oscillatory work when under tension are generally referred to as “stretch activation” of the muscle, for it seems that stretching the muscle in some way activates the cross-bridge cycle.

Various mechanisms have been proposed to account for the nonlinear phenomenon of stretch activation. Thorson and White (1969) proposed a modification of the original Huxley (1957) two-state cross-bridge cycle, suggesting that the rate of cross-bridge attachment was directly proportional to the strain in the thick filaments, whereas Julian (1969)

proposed an alternative modification of Huxley's theory, incorporating an additional exponential process. The reader will find an excellent review of this early work in White and Thorson (1975). Some years later, Thorson and White (1983) modified their model to include changes in the detachment rate due to cross-bridge distortion, but they retained the assumption of strain activation in the thick filaments. Before this work, Wray (1979), following Deschevereskii (1971), proposed a quite different structural model in which stretch activation arose because stretching insect flight muscle brought more actin binding sites into register with the cross-bridges. However, this structural model has been queried by Squire (1992) on the basis of x-ray diffraction experiments.

The above models all assume that the mechanism of stretch activation is special to insect flight muscle. However, Steiger (1977) pointed out that cardiac muscle also displays stretch activation and that negative viscosity is even present to some extent in skeletal muscle. Kawai and Brandt (1980) also observed this effect in several different muscle preparations. It is possible therefore that stretch activation may be a more general nonlinear property of cross-bridges. Indeed, we have shown that even a two-state cross-bridge model (Schoenberg et al., 1984) exhibits striking nonlinear elasticity (Thornhill and Thomas, 1993; Thomas and Thornhill, 1995a). Extending this analysis to a three-state model similar to that discussed by Herzig (1977) and Murase et al. (1986), we showed (Thomas and Thornhill, 1995a,b) that stretch activation and negative viscosity may arise as natural features of the cross-bridge cycle for a cross-bridge interacting with a single attachment site.

The three-state model incorporates thermally activated cross-bridge attachment to stretch the cross-bridge spring (Schoenberg et al., 1984), followed by a power stroke (Huxley, 1969; Huxley and Simmons, 1971) and subsequent detachment. This simple model provides a useful insight

*Received for publication 3 November 1995 and in final form 5 March 1996.*

Address reprint requests to Dr. R. A. Thornhill, School of Biological Sciences, The University of Birmingham, Birmingham B15 2TT, England. Tel.: 121-414-5480; Fax: 121-414-5925; E-mail: r.a.thornhill@bham.ac.uk.

© 1996 by the Biophysical Society

0006-3495/96/06/2807/12 \$2.00

into the possible origin of stretch activation, but inevitably it omits some important features of the cross-bridge cycle. We wish to show in this paper how stretch activation may be produced as a nonlinear property of cross-bridges within a more realistic six-state model for the cross-bridge cycle, similar to that discussed by Rayment et al. (1993) and Cooke (1993). A particular strength of the six-state model is that it distinguishes between weak- and strong-binding cross-bridge states before and after the power stroke. Hence, it takes proper account of the different roles played by inorganic phosphate, ADP, and ATP in the cross-bridge cycle. Indeed, the six-state model may be regarded as a simplification of a scheme originally proposed by A. F. Huxley (1980). In the following sections we describe the model and analyze its response to both oscillatory and stepwise filament displacements. Some of the properties of this model have also been described very briefly elsewhere (Thomas and Thornhill, 1994a,b, 1995c,d).

## THE SIX-STATE CROSS-BRIDGE CYCLE

### Description of the model

Fig. 1 shows a conceptual representation of the six-state cross-bridge cycle. This particular scheme incorporates features of the cross-bridge cycle that have been established by many different experiments, as is discussed by Rayment et al. (1993) and Cooke (1993). The cross-bridge *C* is linked by an ideal spring of stiffness  $\lambda_0$  to the thick filament *A*, and it can attach to the thin filament *B* at a single site *P* by stretching the spring by an amount that is determined by the relative positions of filaments *A* and *B*. We denote the six separate cross-bridge states in this model by numbers 0 to 5. In state 0, the cross-bridge is detached from the filament and has just hydrolyzed ATP, but the products of hydrolysis (ADP and inorganic phosphate  $P_i$ ) are still bound to the myosin head. The detached cross-bridge can bind weakly

and reversibly to the thin filament, forming the short-lived "weak-binding" state 1. Release of inorganic phosphate produces the "strong-binding" state 2, from which the cross-bridge is able to execute its power stroke, thereby stretching the spring by a further amount  $h$  to produce state 3. As shown in Fig. 1, we take the extension of the spring after the power stroke to be  $x$ , and this also serves as a measure of the filament displacement.

The power stroke in Fig. 1 is followed by release of ADP, after which the cross-bridge is in the rigor state 4. The rigor cross-bridge is very strongly bound to the thin filament, but its binding is weakened when a fresh molecule of ATP binds to the myosin head. This leaves the actomyosin complex in state 5 at the end of the cycle. Subsequent dissociation of the actomyosin and rapid hydrolysis of the bound ATP return the cross-bridge to state 0, from which the cycle can start again.

### Role of the cross-bridge spring

We make the same assumptions here about the role of the spring in the cross-bridge kinetics as in our treatment of the three-state cross-bridge model (Thomas and Thornhill, 1995b). The detached cross-bridge in state 0 undergoes thermal Brownian motion, during which the cross-bridge spring is either stretched or compressed. Cross-bridge attachment to the weak-binding state 1 can only occur when the cross-bridge is very close to the attachment site *P*. Hence, for attachment to occur the spring must first be stretched by an amount  $x - h$ , as shown in Fig. 1. Such an extension of the cross-bridge spring requires an elastic energy of  $\lambda_0(x - h)^2/2$ . This energy limits the extent of the Brownian motion of the detached cross-bridge and is obtained as heat from the surroundings. Following Schoenberg et al. (1984), we therefore regard cross-bridge attachment as a thermally activated process, and we write the rate constant for attachment as

$$k_{01}(x) = k_{01}e^{-\lambda_0(x-h)^2/2kT}, \quad (1)$$

where  $k_{01}$  is the attachment rate when the filament displacement  $x = h$ ,  $k$  is Boltzmann's constant, and  $T$  is the absolute temperature of the surrounding fluid. Note that the extension  $x - h$  is negative when  $x < h$ . This corresponds to the case where the attachment site *P* in Fig. 1 is to the left of the equilibrium position of the detached cross-bridge, so that the spring must be compressed rather than stretched for the cross-bridge to attach at *P*. We show in the following sections that such compression of the cross-bridge spring at the start of the cycle is actually a fundamental factor in producing stretch activation.

At thermal equilibrium, the cross-bridge undergoes continual random attachment and detachment. In contrast to Eq. 1, the detachment rate constant  $k_{10}$  is assumed to be independent of filament displacement, because stretching the spring does not affect the energy needed to detach the cross-bridge, provided the link to the thin filament is rigid.

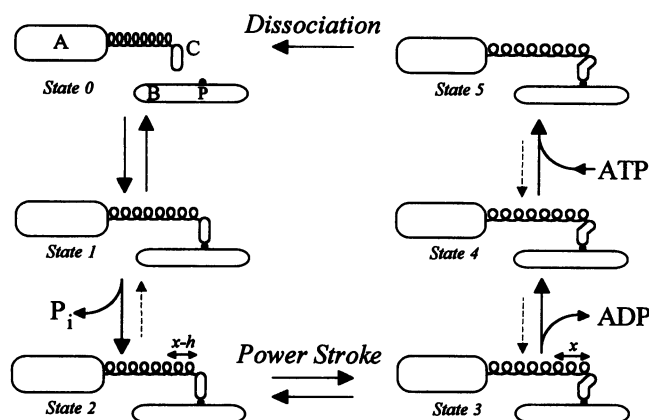


FIGURE 1 Schematic diagram of the six-state cross-bridge model. The cross-bridge *C* is linked to a thick filament *A* by a spring, and it can attach to the thin filament *B* at a single site *P*. The length of the power stroke is denoted by  $h$ , whereas  $x$  is the extension of the spring at the end of the power stroke and serves as a measure of the filament displacement.

Strictly speaking, this can only be approximately true. In practice, there must be some compliance in the link, so the attachment angle will change slightly when the spring is under tension, and the elastic energy stored in the link will promote cross-bridge detachment. However, we shall assume here that the link is much stiffer than the cross-bridge spring. In that case, the elastic energy stored in the link is much less than that in the series spring, and we may neglect it to a first approximation. Essentially the same approximation has been used by Schoenberg et al. (1984) in discussing a two-state model for cross-bridges in relaxed muscle.

The transition from state 2 to state 3 represents the cross-bridge power stroke, which stretches the spring by a further amount  $h$ . The change in elastic energy affects the rate constants for this step in the cross-bridge cycle, and at thermal equilibrium we find that

$$k_{23}(x)/k_{32}(x) = k_{23}e^{-\lambda_0 x h/kT}/k_{32}, \quad (2)$$

where  $k_{23}$  and  $k_{32}$  are the respective rate constants for forward and backward tilting of the cross-bridge when the filament displacement  $x = 0$ . Following Huxley and Simmons (1971), we assume that only the forward rate is actually affected by the elastic energy, in which case

$$k_{23}(x) = k_{23}e^{-\lambda_0 x h/kT}, \quad (3a)$$

$$k_{32}(x) = k_{32}. \quad (3b)$$

In principle, we should also consider  $k_{05}(x)$ , the rate constant for the detached cross-bridge to reattach in state 5, which is given by

$$k_{05}(x) = k_{05}e^{-\lambda_0 x^2/2kT}, \quad (4)$$

where  $k_{05}$  is the attachment rate when  $x = 0$ . We argue below that this extremely slow process may be neglected in practice for cross-bridges in active muscle.

As with the detachment rate constant  $k_{10}$  from the weak-binding state, we make the simplifying assumption here that the rate constant  $k_{50}$  for dissociation at the end of the cross-bridge cycle is independent of filament displacement. Note, however, that Nishizaka et al. (1995) have studied the very slow dissociation from the rigor state 4 for actomyosin in the absence of ATP. They observed an increase in the rigor dissociation rate at filament displacements of about 20 nm, when the spring tension was about 10 pN. This situation may actually occur physiologically during rapid stretches of muscle (Curtin and Davies, 1973; Flitney and Jones, 1990; Campbell and Lakie, 1996). However, we show in the following section that, under nearly isometric conditions, cross-bridges in active muscle cannot readily tilt over to exert high rigor tensions, because the power stroke is inhibited by the large elastic energy in Eq. 3. We therefore restrict our analysis in this paper to low cross-bridge tensions, where the detachment rate constants are assumed to be independent of filament displacement. In that case, Eqs. 1, 3, and 4 serve to couple the cross-bridge kinetics to the filament displacement  $x$  in a very simple way.

## Thermodynamic considerations

The cross-bridge cycle is not in thermodynamic equilibrium under normal physiological conditions, owing to the continuous hydrolysis of ATP, as indicated in Fig. 1. However, the rate constants must nonetheless be chosen so that the cross-bridge model does not in principle violate thermodynamics (Chen and Brenner, 1993). If the system were in thermodynamic equilibrium, then according to Einstein's principle of detailed balance (Reif, 1965), the forward and backward rates for each step in the cross-bridge cycle would be equal. Each of these rates is the product of a rate constant and the appropriate occupation probability for the cross-bridge state. Hence we find that the rate constants at thermodynamic equilibrium must obey the relation

$$k_{01}(x)k_{12}k_{23}(x)k_{34}k_{45}k_{50} = k_{05}(x)k_{54}k_{43}k_{32}(x)k_{21}k_{10}. \quad (5)$$

The exponential terms in Eqs. 1, 3, and 4 ensure that this equality can be satisfied for all values of  $x$ . Hence the ATP hydrolysis rate at thermodynamic equilibrium is zero, independent of filament displacement  $x$ . This is an essential requirement for any cross-bridge model. Note that Eqs. 1, 3, and 4 specify the explicit temperature dependence that arises from the elastic energy, but the rate constants themselves may also depend implicitly on temperature, pH, and ionic strength.

The rate constant  $k_{45}$  for ATP binding on the left-hand side of Eq. 5 is proportional to [ATP], whereas  $k_{43}$  and  $k_{21}$  on the right-hand side are proportional to [ADP] and  $[P_i]$ , respectively. For 1 mM concentrations of ADP and  $P_i$ , the equilibrium ATP concentration is about  $10^{-8}$  mM. If the rate constant for ATP binding is taken to be  $4 \times 10^3 \text{ mM}^{-1} \text{ s}^{-1}$  (Finer et al., 1994), this implies an equilibrium value for  $k_{45}$  of only  $4 \times 10^{-5} \text{ s}^{-1}$ . This very small equilibrium value for  $k_{45}$  must be balanced by a comparable term on the right-hand side of Eq. 5. We assume here that it is the reattachment rate constant  $k_{05}$  that is very small, which amounts to saying that the final dissociation and hydrolysis step in Fig. 1 is essentially irreversible. The equilibrium value of  $k_{05}$  is therefore so small that one can set  $k_{05} = 0$  in the kinetics with very little error. In contrast, we treat the release of phosphate and ADP as reversible processes, because it has been found that increasing  $[P_i]$  or [ADP] has an appreciable effect on the cross-bridge cycle (White and Thorson, 1972; Thirlwell et al., 1994; Horiuti et al., 1994; Thomas and Thornhill, 1995c).

## Choice of parameters

There are 14 parameters in the six-state model. For the purposes of illustration we have chosen their values to be  $h = 10 \text{ nm}$ ,  $\lambda_0 = 0.2 \text{ pN nm}^{-1}$ ,  $k_{01} = 20 \text{ s}^{-1}$ ,  $k_{10} = 1000 \text{ s}^{-1}$ ,  $k_{12} = 10000 \text{ s}^{-1}$ ,  $k_{21} = 5 \text{ s}^{-1}$ ,  $k_{23} = 5000 \text{ s}^{-1}$ ,  $k_{32} = 100 \text{ s}^{-1}$ ,  $k_{34} = 100 \text{ s}^{-1}$ ,  $k_{43} = 5 \text{ s}^{-1}$ ,  $k_{45} = 500 \text{ s}^{-1}$ ,  $k_{54} = 5 \text{ s}^{-1}$ ,  $k_{50} = 500 \text{ s}^{-1}$ , and  $k_{05} = 0$ . In choosing these values, we were guided by the following considerations.

1. In relaxed muscle, where phosphate release is slow owing to the absence of calcium activation, cross-bridges readily detach from the weak-binding state. We have taken the ratio  $k_{10}/k_{01}$  to be 50, which means that only a small fraction (about 2%) of cross-bridges in relaxed muscle would be attached at steady state.

2. Calcium activation catalyzes phosphate release in active muscle (Rayment et al., 1993). We have taken  $k_{12}/k_{10} = 10$ , so that a weakly bound cross-bridge in active muscle is much more likely to release phosphate than to detach from the thin filament. The transition from the weak-binding state 1 to the strong-binding state 2 therefore occurs very rapidly, and the lifetime of the weak-binding state 1 in active muscle is extremely short. It also follows that most cross-bridges before the power stroke in active muscle will be found in the strong-binding state.

3. The rate constant  $k_{21}$  for phosphate rebinding has been chosen to be fairly low here, corresponding to a low concentration of free phosphate. Note that detachment from the strong-binding state 2 is a composite process, in which the cross-bridge must first rebind phosphate and then detach from the weak-binding state. The effective detachment rate constant for this process is therefore  $k_{21}k_{10}/(k_{10} + k_{12})$ . This corresponds to the very low value of  $k_{10} = 0.455 \text{ s}^{-1}$  used for the detachment rate in the simplified three-state model (Thomas and Thornhill, 1995b). The six-state model presents a much clearer picture of the important role that phosphate plays in the cross-bridge cycle.

4. Forward tilting in the power stroke must be very fast to account for the rapid tension transients observed in quick-release experiments similar to those of Huxley and Simmons (1971).

5. Release of ADP is slower than phosphate release (Finer et al., 1994). State 3 after the power stroke is therefore longer lived than the weak-binding state 1.

6. Binding of ATP is rapid, provided, of course, that sufficient ATP is available (Finer et al., 1994).

7. Dissociation of state 5 after binding ATP is also rapid. Hence, ADP release represents a "bottleneck" that limits the rate of dissociation after the power stroke. Note, however, that our simulation of the effect of ADP on the response of rigorized cross-bridges to the release of caged ATP (Thomas and Thornhill, 1995c), as in the experiment of Thirlwell et al. (1994), required the dissociation of state 5 to be much slower.

Our choice of parameters leads to behavior that compares reasonably well with the properties of fibrillar insect flight muscle (Thomas and Thornhill, 1994a). However, it should be borne in mind that the actual values of basic quantities such as the length of the power stroke  $h$  and the stiffness of the cross-bridge spring  $\lambda_0$  are the subject of considerable uncertainty. Recent experiments on actomyosin from different groups have yielded very different values for these parameters (Finer et al., 1994; Ishijima et al., 1994; Molloy et al., 1995; Nishizaka et al., 1995).

## Cross-bridge rate equations

The kinetics of the six-state cross-bridge model are determined by the following rate equations for the occupation probabilities of the states in Fig. 1:

$$dp_1/dt = k_{01}(x)p_0 - (k_{10} + k_{12})p_1 + k_{21}p_2, \quad (6a)$$

$$dp_2/dt = k_{12}p_1 - (k_{21} + k_{23}(x))p_2 + k_{32}p_3, \quad (6b)$$

$$dp_3/dt = k_{23}(x)p_2 - (k_{32} + k_{34})p_3 + k_{43}p_4, \quad (6c)$$

$$dp_4/dt = k_{34}p_3 - (k_{43} + k_{45})p_4 + k_{54}p_5, \quad (6d)$$

$$dp_5/dt = k_{45}p_4 - (k_{50} + k_{54})p_5 + k_{05}(x)p_0, \quad (6e)$$

where  $p_0 = 1 - (p_1 + p_2 + p_3 + p_4 + p_5)$ . Note that we have used the fact that the sum of the occupation probabilities for the six states in the cycle must add up to unity, so that there are only five independent rate equations. These equations determine both the steady-state properties and the elastic response of the six-state cross-bridge model, as we show in the following sections.

## STEADY-STATE BEHAVIOR

### Steady-state tension

At steady state, the time derivatives in the cross-bridge rate equations (Eqs. 6a–e) are zero, and we are left with five simultaneous equations that determine the occupation probabilities. Their algebraic solution for the simple case where  $k_{05} = 0$  is given in Appendix I, whereas Fig. 2 illustrates the resultant steady-state behavior with the model parameters chosen as above. The average tension  $f$  is shown as the heavy line in Fig. 2 A. Algebraically, it is given by the expression

$$f = f_{12} + f_{345} = \lambda_0(x - h)(p_1 + p_2) + \lambda_0x(p_3 + p_4 + p_5), \quad (7)$$

where  $f_{12}$  and  $f_{345}$  are the respective contributions from attached cross-bridges before and after the power stroke. These two components are represented by the light line and the dashed line in Fig. 2 A. Note that  $f_{12}$  is negative for  $x < h$  because the cross-bridge spring is then in compression in states 1 and 2 before the power stroke. Two notable features of the curve for the average tension  $f$  are the broad peak in the region of  $x = 20 \text{ nm}$ , indicative of a mechanical yield point (Thomas and Thornhill, 1995a), and the virtual absence of any tension for  $x < 0$ . The asymmetry of the tension curve for positive and negative filament displacements is a reflection of the ratchet-like behavior of cross-bridges.

### Stretch activation

Fig. 2 B shows the variation of the cross-bridge attachment probabilities with filament displacement  $x$ . We show the

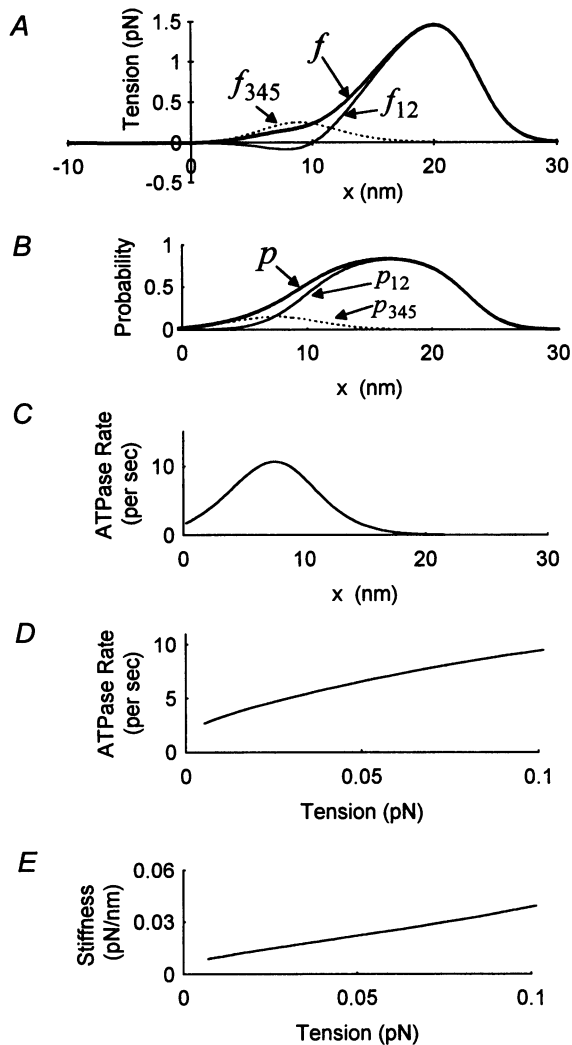


FIGURE 2 Equilibrium behavior of the six-state model as a function of filament displacement  $x$ . (A) Behavior of the average tension  $f$  (heavy line) together with the contributions  $f_{12}$  from states 1 and 2 before the power stroke (light line) and  $f_{345}$  from states 3, 4, and 5 after the power stroke (dashed line). (B) Variation of the attachment probabilities  $p_{12}$  and  $p_{345}$  and their sum  $p$ . (C) The ATPase rate indicates stretch activation along the rising part of the tension curve in A up to  $x = 8$  nm. (D and E) Variation of the ATPase rate and high-frequency stiffness as a function of tension in the region of stretch activation.

probabilities  $p_{12} = p_1 + p_2$  and  $p_{345} = p_3 + p_4 + p_5$  for the cross-bridge to be attached before and after the power stroke, together with the total attachment probability  $p = p_{12} + p_{345}$ . At small values of  $x$ , we find that  $p_{12} \ll p_{345}$ , because the cross-bridge rapidly releases its inorganic phosphate and executes the power stroke. The cross-bridge spring in this case is strongly compressed before the power stroke. The attachment probabilities therefore increase with filament displacement  $x$ , because increasing  $x$  relieves the spring compression and hence reduces the elastic energy required for attachment. This in turn increases the attachment rate constant  $k_{01}(x)$  given by Eq. 1.

The increase in the attachment rate with increasing filament displacement produces an increase in the overall turnover rate for the cross-bridge cycle. This rate is the same as the dissociation rate  $k_{50}p_5$  at the end of the cycle, because the net rate for each of the steps in Fig. 1 must be equal at steady state. Furthermore, it must also be equal to the steady-state rate of ATP hydrolysis, on the assumption that one ATP molecule is hydrolyzed per cycle. Fig. 2 C accordingly shows the steady-state ATPase rate as a function of filament displacement. One can see that the ATPase rate increases for small filament displacements up to a peak of about  $10 \text{ s}^{-1}$  at  $x = 8$  nm. Since increasing the filament displacement  $x$  corresponds to stretching real muscle, we may say that the cross-bridge exhibits stretch activation for filament displacements from zero to 8 nm.

Fig. 2 D shows another way to view the stretch activation. Here we have plotted the ATPase rate as a function of tension in the region of stretch activation. The ATPase rate increases roughly linearly with tension, as is in fact observed experimentally (Rüegg and Tregear, 1966; Rüegg and Stumpf, 1969). A similar linear variation is found for the high-frequency stiffness (which is shown in the following section to be  $\lambda_0 p$ ) shown in Fig. 2 E, and this behavior has also been observed experimentally (Herzig, 1977; White et al., 1977). Note that, although the ATPase rate increases as a function of bias tension, the cross-bridge is not performing any net mechanical work here, because the filament displacement is static. This corresponds to isometric conditions in a real muscle sample. The chemical energy released in the ATP hydrolysis is therefore dissipated as heat.

### Trapping in the strong-binding state

Stretch activation only occurs along the lower part of the tension curve in Fig. 2 A. One can see from Fig. 2 C that the ATPase rate decreases at higher filament displacements, whereas the tension continues to rise up to the yield point at about 20 nm. The continued rise of tension is due to the increase in  $f_{12}$ , representing the contribution from states 1 and 2 before the power stroke. Indeed, Fig. 2 B shows that the attachment probability  $p_{12}$  also increases to a peak for large filament displacements. In fact, the cross-bridge tends to get trapped in the strong-binding state 2 before the power stroke (Thomas and Thornhill, 1995d).

Trapping in the strong-binding state is due to two factors. First of all, Eq. 3 implies that the rate constant for the power stroke decreases for large filament displacement  $x$  because of the increase in the elastic energy required to stretch the spring. Thus it becomes more and more difficult for a cross-bridge in state 2 to tilt over into state 3. Second, we have also assumed that the rate constant  $k_{21}$  for restoration of the weak-binding state 1 by rebinding inorganic phosphate in state 2 is rather low. Hence the effective rate constant  $k_{21}k_{10}/(k_{10} + k_{12})$  for detachment from the strong-binding state is also very low. The result is that the cross-

bridge becomes virtually locked in the strong-binding state 2 for large values of  $x$ .

The trapping effect is even more pronounced if we further decrease the rate constant  $k_{21}$ , which corresponds to decreasing the concentration of inorganic phosphate. This may be related to the "phosphate starvation" effect observed by White and Thorson (1972) in fibrillar insect flight muscle. Increasing  $k_{21}$ , which is equivalent to adding phosphate, decreases the size of the tension peak, but only has a small effect in the region of stretch activation.

### Comparison with skeletal muscle

We have assumed here that a cross-bridge under nearly isometric conditions interacts predominantly with a single actin-binding site. Abbott and Cage (1978) found some evidence for this in fibrillar insect flight muscle in the form of a 38.5-nm periodicity in the response to large-amplitude slow stretches. This periodicity corresponds to the helical repeat of the thin filament, and a similar periodicity has been observed more recently in an actomyosin preparation by Molloy et al. (1995). In contrast, to model skeletal muscle one needs to take account of attachment sites on successive actin monomers (Slawnych et al., 1994). Because the spacing of actin monomers is only 5.46 nm, the Brownian motion of a detached cross-bridge may allow it to interact with several nearby attachment sites, even under isometric conditions.

Dantzig et al. (1992) have studied the effect of phosphate release on skeletal rabbit psoas muscle. They found that increasing  $[P_i]$  decreases the isometric tension in a way similar to that of the decrease in the tension peak in Fig. 2 A. However, they interpreted this as a reversal of the power stroke due to phosphate binding, whereas we would suggest that it may be due to reduced trapping in the strong-binding state. We would expect such trapping to occur in skeletal muscle with low  $[P_i]$  at any filament position owing to attachment sites with large  $x$ , which are to the right of  $P$  in Fig. 1. Our Monte Carlo simulations (Thomas and Thornhill, 1995d) show that cross-bridges may become trapped in the strong-binding state after attaching to these sites, leaving the spring under a large tension. Hence, the strongly attached cross-bridges will make a large contribution to the average isometric tension exerted by the cross-bridges. Adding phosphate reduces the number of strongly bound cross-bridges, and hence the isometric tension is also reduced. Note, however, that we would expect relatively little change in the ATPase rate, which is mainly due to sites with smaller  $x$ -values (in fact, in the region of stretch activation in Fig. 2), where the cross-bridges can tilt over easily.

## ELASTICITY

### Cross-bridge elastic constant

The elastic response of the six-state cross-bridge model can be analyzed by introducing a small oscillatory displacement

$\delta x$  at angular frequency  $\omega$  into Eqs. 6a–e. Neglecting terms in  $\delta x^2$  and making use of the complex representation for the oscillation, we find that Eq. 6a may be rewritten as

$$j\omega\delta p_1 = -\delta p_1/\tau_1 - k_{01}(x)(\delta p_2 + \delta p_3 + \delta p_4 + \delta p_5) + k_{21}\delta p_2 + p_0\delta x dk_{01}(x)/dx, \quad (8)$$

where  $\delta p_1$  is the complex amplitude of the oscillatory component in the occupation probability  $p_1$ . We can write down similar equations for the other probabilities and solve the resultant simultaneous equations to determine  $\delta p_1$ , etc. The algebra for this is rather complicated, so we have consigned the details to Appendix II.

The amplitude of the oscillatory tension is easily shown by taking differentials of Eq. 7 to be

$$\delta f = \lambda_0(x - h)(\delta p_1 + \delta p_2) + \lambda_0 x(\delta p_3 + \delta p_4 + \delta p_5) + \lambda_0(p_1 + p_2 + p_3 + p_4 + p_5)\delta x. \quad (9)$$

Hence the frequency-dependent complex elastic constant of the cross-bridge is

$$\lambda(\omega) = \lim_{\delta x \rightarrow 0} \left( \frac{\delta f}{\delta x} \right). \quad (10)$$

At zero frequency the elastic constant is just the slope  $df/dx$  of the tension curve in Fig. 2 A. One can see that this slope increases in the region of stretch activation, although it decreases at higher filament displacements and is in fact negative in the mechanically unstable region beyond the yield point.

In the high-frequency limit, the occupation probabilities cannot respond rapidly enough to the oscillating displacement  $\delta x$ , so we may set  $\delta p_1 = 0$ , etc. In that case, one can see from Eq. 9 that the high-frequency elastic constant, or stiffness, is given by

$$\lambda(\infty) = \lambda_0(p_1 + p_2 + p_3 + p_4 + p_5) = \lambda_0 p. \quad (11)$$

In other words, the high-frequency stiffness is a direct measure of the total attachment probability  $p$ , a fact that is often used in muscle experiments. Fig. 2 E shows that the high-frequency stiffness increases with tension as the attachment probability increases in the region of stretch activation.

### Nyquist plots

The frequency-dependent elastic constant  $\lambda(\omega)$  for  $x = 4$  nm is represented graphically in Fig. 3 A in the form of a Nyquist plot, as used, for instance, by Machin and Pringle (1959), White and Thorson (1975), Kawai and Brandt (1980), and Murase et al. (1986). The Nyquist trajectory is a plot of the imaginary part of  $\lambda(\omega)$  against its real part, in this case from 0 Hz to 1 kHz. The real part represents the in-phase, or elastic, response of the tension produced by the oscillatory displacement  $\delta x$ , whereas the imaginary part

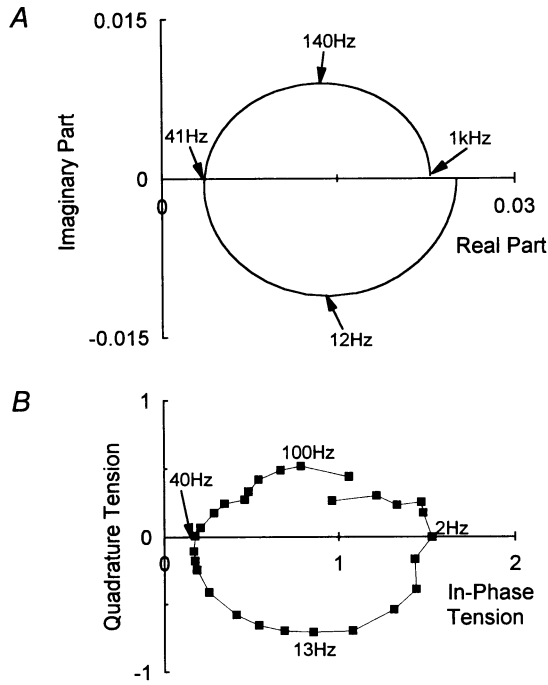


FIGURE 3 Theoretical and experimental Nyquist plots. (A) Theoretical Nyquist plot for a single cross-bridge in the six-state model when  $x = 4$  nm. (B) An experimental Nyquist plot for a bundle of glycerinated fibres from *Lethocerus indicus* (Thomas and Thornhill, 1994b).

represents the quadrature component of the tension, which is a measure of the viscous response of the system. One can see from Fig. 3 A that the cross-bridge has a normal, positive, viscous response at frequencies above 41 Hz, reaching a maximum at 140 Hz. In contrast, the viscous response is negative below 41 Hz, reaching a maximum negative value at 12 Hz. Hence the cross-bridge displays negative viscosity below 41 Hz.

By way of comparison, Fig. 3 B shows an experimental Nyquist plot that we obtained for a bundle of glycerinated fibers of fibrillar insect flight muscle taken from a giant water bug *Lethocerus indicus* (Thomas and Thornhill, 1994b). Similar behavior has been observed by Jewell and Rüegg (1966). The real muscle exhibits negative viscosity below 40 Hz, and the general similarity with the theoretical curve in Fig. 3 A is very striking.

Fibrillar insect flight muscle only displays appreciable negative viscosity when the muscle is under a steady bias tension. This aspect of stretch activation is also present in the theoretical model and is illustrated in Fig. 4, which shows a series of theoretical Nyquist plots for different values of the filament displacement  $x$  in the range 0 to 8 nm. There is no negative viscosity, and indeed very little loss at all, when  $x = 0$  nm, but a small negative-viscosity loop is just visible for  $x = 1$  nm. This negative-viscosity loop grows rapidly with tension up to  $x = 7$  nm. Beyond this, the high-frequency loop becomes more prominent, and, as the filament displacement is increased further, the high-frequency loss loop grows at the expense of the low-frequency negative viscosity.

At  $x = 20$  nm (not shown in Fig. 4), there is no negative viscosity, and the Nyquist plot looks like that for a two-state system (Thomas and Thornhill, 1995a). The two-state system arises here because the cross-bridge spends most of its time trapped in the strong-binding state but occasionally manages to detach from the filament via the weak-binding state. It almost never executes the power stroke, owing to the large elastic energy in Eq. 3. The strain-induced detachment at high rigor tensions observed by Nishizaka et al. (1995) may therefore not be important in active muscle. We find that the zero-frequency stiffness at  $x = 20$  nm is practically zero, and it becomes negative in the mechanically unstable region beyond the yield point.

### Isotonic instability

Fig. 4 also provides an indication of another potential mechanical instability that occurs within the region of stretch activation. One can see that the Nyquist loop encircles the origin for filament displacements above 4 nm. Under strictly isometric conditions this would not be significant, as the origin simply represents a zero in the response function in Eq. 10. However, the situation is very different if we consider a cross-bridge held under isotonic conditions (that is, under a constant load rather than at a constant filament displacement). In that case, the origin represents a pole (that is, an infinity) in the mechanical compliance, and one would expect that an isotonic system whose Nyquist plot encircles this pole would tend to oscillate spontaneously. Such oscillations are a consequence of the intrinsic mechanical instability of cross-bridges and do not require the presence of a mechanical resonator, as in the work of Machin and Pringle (1959).

One can achieve nearly isotonic conditions by placing a weak spring in series with a muscle. As we have discussed briefly elsewhere (Thomas and Thornhill, 1996), this system would exhibit spontaneous tension oscillations, even under isometric conditions provided that 1) the Nyquist plot for the muscle encircles the origin and 2) the stiffness of the series spring is less than the value where the Nyquist plot for the muscle crosses the negative real axis. We have also shown that a vestige of these oscillations is present in the transient response of the system, even in the presence of a stronger series spring, which stabilizes the system. This may account for the tension oscillations that are sometimes seen in quick-stretch experiments with glycerinated fibrillar insect flight muscle and cardiac muscle (Steiger, 1977). Such a situation may not normally occur in intact flight-muscle preparations, where the presence of parallel elastic components tends to stabilize the system by adding to the cross-bridge stiffness and shifting the Nyquist plots in Fig. 4 to the right (D. C. S. White, private communication).

An important potential source of series elasticity is the muscle filaments themselves. Higuchi et al. (1995) have recently shown that the thin filaments in rabbit skeletal muscle have a significant compliance, as had previously been inferred from high-resolution x-ray diffraction (Hux-

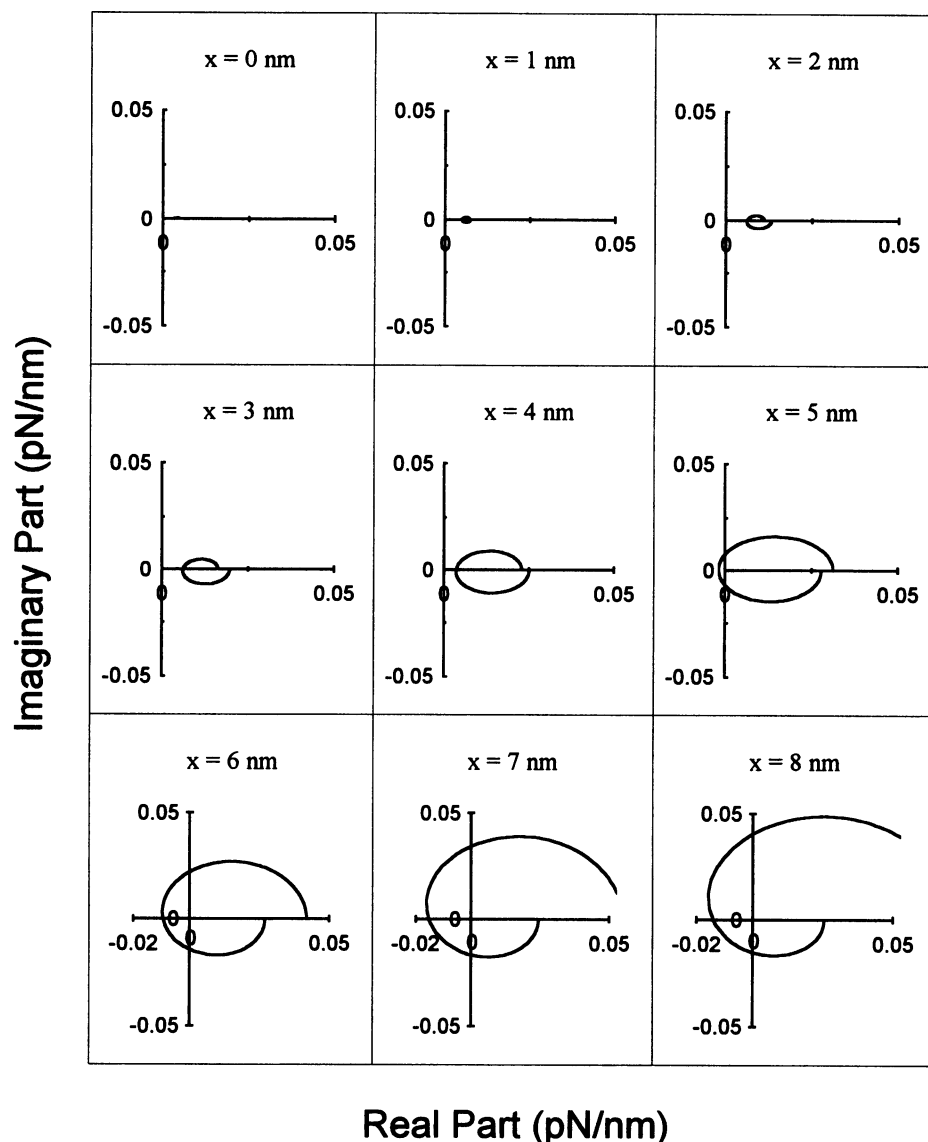


FIGURE 4 Stretch activation for the six-state model showing Nyquist plots for filament displacement  $x$  varying from 0 to 8 nm. The negative-viscosity loop grows with bias tension as  $x$  increases from 1 to 5 nm. At larger displacements the high-frequency loop grows and it progressively moves to lower frequencies.

ley et al., 1994; Wakabayashi et al., 1994). However, thin-filament compliance may be less important in fibrillar insect flight muscle, because this type of muscle has a very narrow I-band. We have therefore omitted filament compliance from the calculations in this paper.

### Structural relaxation

It is rather surprising that the mechanical response in Fig. 3 *B* for a fiber bundle should be so similar to that for a single cross-bridge in Fig. 3 *A*. The periodicities of the actin and myosin filaments are, after all, quite different, and so one would expect the cross-bridges in real muscle to display a wide range of  $x$  values. We have suggested that the apparent narrow range of  $x$  values may be the result of structural relaxation (or "creep") in the cross-bridge spring (Luo et al., 1993; Thomas and Thornhill, 1995b,e). Such structural relaxation would cause each cross-bridge spring to increase its

rest length in proportion to the average tension in the spring. Hence, cross-bridges with large  $x$  values would develop springs with longer rest lengths, reducing considerably the effective range of  $x$  values. This process may play an important regulatory role in real muscle specimens, because the cross-bridges in insect flight muscle would all have similar Nyquist plots and would therefore be better placed to perform their oscillatory work in unison.

Structural relaxation has been observed in rigorized muscle (Steiger, 1977; Thomas et al., 1993) and in the presence of ATP analogs (Schoenberg and Eisenberg, 1985). It introduces an additional loss process into the muscle at very low frequencies. We have suggested that this may be the origin of the low-frequency loss loop present below 2 Hz in the experimental Nyquist plot for real muscle in Fig. 3 *B* (Thomas and Thornhill, 1995e). However, for simplicity, we have omitted this additional relaxation process from the present theoretical analysis.

A corollary of the above argument is that an additional series elastic element may also extend the range of muscle lengths over which stretch activation can occur. When a muscle is stretched, part of the extension will be taken up by the series elastic element so that the change in filament displacement  $x$  is reduced. Indeed, Huxley et al. (1994) have suggested that this may occur in skeletal muscle owing to the compliance of the thin filaments. Structural relaxation in the cross-bridge spring would also effectively reduce the change in  $x$ . We have shown that the range of stretch activation with a 10-nm power stroke is about 8 nm, which corresponds to a less than 1% change in muscle length. Series compliance may usefully extend this range.

## RESPONSE TO A LENGTH STEP

### Stretch activation and the delayed tension

Many investigators (for instance, Huxley and Simmons, 1971; White and Thorson, 1975; Herzig, 1977) use large ( $\sim 5$ – $10$  nm) length steps rather than small sinusoidal displacements when measuring the mechanical response of muscle. It is straightforward to adopt the same approach in our theoretical model by introducing a step in the filament displacement  $x$  into Eqs. 6a–e. These equations are then integrated numerically on a computer using a Runge-Kutta algorithm.

Fig. 5 A illustrates the response of a cross-bridge to a 5-nm-length step applied at  $t = 10$  ms, starting from an initial filament displacement of zero. There is a small instantaneous rise in the tension as soon as the length step is applied, indicating that the initial high-frequency elasticity at  $x = 0$  nm is very small, as one can also infer from Fig. 2 E. The initial rise is followed by a rapid decay, analogous to the rapid tension transients studied by Huxley and Simmons (1971). However, the rapid decay in tension is followed by a much slower tension rise, which is generally referred to as the “delayed tension.” This phase is particularly prominent in fibrillar insect flight muscle, although it is also found in other types of muscle (Steiger, 1977). From a physical point of view, the delayed rise in tension is very curious, as one generally expects a tension transient to decay rather than to grow. This contrary behavior is a reflection of the negative viscosity in the Nyquist plots of Fig. 4, whereas the initial rapid decay in the tension transient corresponds to the high-frequency loop, which has a normal positive loss. Tension transients similar to Fig. 5 A are generally regarded as a direct demonstration of stretch activation.

Fig. 5 B shows that the delayed tension is accompanied by a rise in the high-frequency stiffness. The steady rise in the stiffness in Fig. 5 B is mainly due to the increase in the attachment probability  $p_{345}$  after the stretch, as in Fig. 2 B. The delayed tension is therefore associated with a slow build-up of attached cross-bridges. In fact, one can see that the stiffness in Fig. 5 B starts to rise immediately after the length step and slightly leads the tension. This lead of

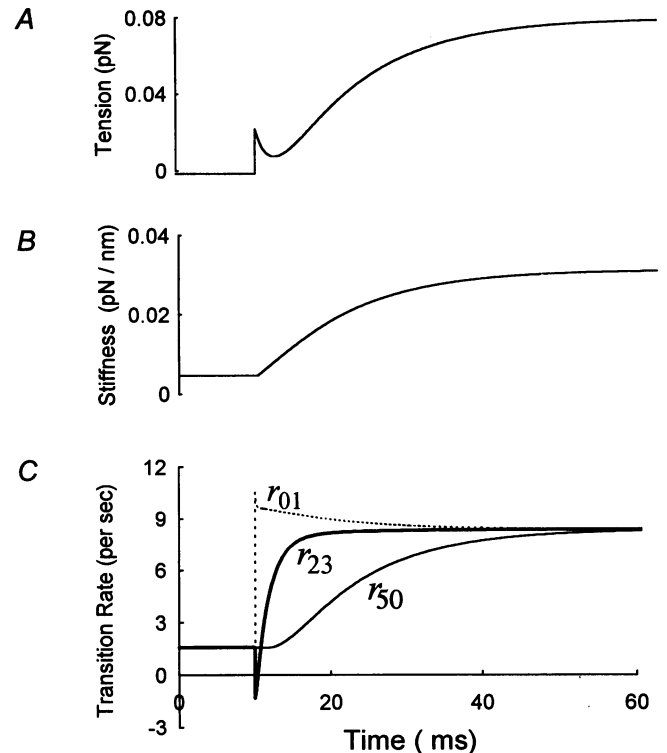


FIGURE 5 Response to a sudden 5-nm stretch, illustrating delayed tension and stretch activation. (A) Time dependence of the tension. The instantaneous rise at  $t = 10$  ms is followed by a rapid decay and then a slow delayed rise. (B) How the high-frequency stiffness rises in response to the stretch. (C) The variation of three of the transition rates in the six-state model.

stiffness over tension is due to the contribution from states 1 and 2, which respond extremely rapidly to the length step.

### Transition rates

A more detailed view of the delayed tension is provided by looking at the transition rates between the different cross-bridge states (Thomas and Thornhill, 1995a). Fig. 5 C shows the variation of three of these rates given by

$$r_{01} = k_{01}(x)p_0 - k_{10}p_1, \quad (12a)$$

$$r_{23} = k_{23}(x)p_2 - k_{32}p_3, \quad (12b)$$

$$r_{50} = k_{50}p_5. \quad (12c)$$

The rate  $r_{01}$  (denoted by the dashed curve in Fig. 5 C) is the net rate of attachment in the weak-binding state at the beginning of the cross-bridge cycle. This rate increases instantaneously in response to the length step, because the step increases the attachment rate constant  $k_{01}(x)$  in Eq. 1. The increased attachment rate is a direct illustration of the phenomenon of stretch activation, and it arises because the 5-nm stretch reduces the initial compression in the cross-bridge spring. The net rate for forward tilting in the power stroke is  $r_{23}$  (denoted by the heavy curve in Fig. 5 C). The stretch causes an instantaneous decrease in  $r_{23}$ , because

$k_{23}(x)$  in Eq. 3 is reduced, owing to the increase in elastic energy required to stretch the spring during the power stroke. Indeed, one can see from Fig. 5 C that  $r_{23}$  is briefly negative immediately after the length step, which means that the stretch inhibits the power stroke to such an extent that it is initially driven into reverse. However, the reduction in  $k_{23}(x)$  is quickly offset by an increase in the occupation probability  $p_2$  for the strong-binding state, which is a consequence of the increased attachment rate  $r_{01}$ . The result is that the cross-bridge tilting rate  $r_{23}$  recovers very rapidly and comes almost into balance with the enhanced attachment rate by about 10 ms after the length step.

In contrast to the tilting rate, the dissociation rate  $r_{50}$  from state 5 at the end of the cross-bridge cycle responds much more slowly to the length step. This rate is represented by the medium-weight curve in Fig. 5 C. There is hardly any change in  $r_{50}$  for the first few milliseconds after the length step, because we have assumed that the detachment rate constant  $k_{50}$  is independent of  $x$ . Hence the dissociation rate only responds to changes in the occupation probability  $p_5$ . (Note that we have assumed here that the rate constant  $k_{34}$  for ADP release is smaller than  $k_{45}$  and  $k_{50}$ , so in fact the real bottleneck after the power stroke will be state 3.) The result is that  $p_5$  increases steadily until the dissociation rate  $r_{50}$  balances the enhanced attachment and tilting rates  $r_{01}$  and  $r_{23}$ . All three rates in Fig. 5 C are ultimately equal at steady state, and the increased turnover rate for the cross-bridge cycle implies that the ATPase rate is also enhanced by the stretch, as in Fig. 2 C.

### The origin of negative viscosity

As with the simple three-state model (Thomas and Thornhill, 1995a), Fig. 5 also provides us with some insight into the origin of the negative viscosity that is so important in fibrillar insect flight muscle. The negative viscosity in Figs. 3 and 4 implies that tension lags the sinusoidal displacement, and this is closely related to the delayed tension effect. (Strictly speaking, the correspondence is only true in the limit of very small length steps, but we find in fact that the small-signal response is broadly similar to the large-amplitude case in Fig. 5 within the region of stretch activation.) When flight muscle is stretched suddenly, the cross-bridge attachment rate and the rate of executing the power stroke come into balance very quickly, but it takes longer for dissociation at the end of the cycle to catch up with the increased rate of throughput. This causes a slow build-up of the number of cross-bridges exerting tension after the power stroke, and it is this lag that is responsible both for the delayed tension and for the negative viscosity.

### CONCLUDING REMARKS

The six-state model (Rayment et al., 1993; Cooke, 1993) is a significant step toward a realistic model for muscle cross-bridges interacting with a single attachment site under nearly isometric conditions. Attachment and detachment at

the start of the cross-bridge cycle are treated as in a two-state model, and we have assumed that the power stroke is also thermally activated, as suggested by Huxley and Simmons (1971). The other steps in the cycle involve binding of ATP and the subsequent release of the products of hydrolysis. The six-state model therefore provides a more realistic picture than the simplified three-state model (Herzig, 1977; Thomas and Thornhill, 1995a) of the steps through which ATP hydrolysis drives the cross-bridge cycle. The coupling of the cross-bridge kinetics to the filament displacement  $x$  via Eqs. 1 and 3 is particularly simple, and the model displays many of the characteristics of fibrillar insect flight muscle.

In the first place, we find that the ATP hydrolysis rate increases with tension for filament displacements up to about 8 nm. Hence the six-state model exhibits stretch activation of the ATPase. An important feature of the six-state model, which is also present in the three-state model, is that stretch activation occurs when the cross-bridge spring is in compression rather than tension at the start of the power stroke. Pulling the filaments relieves the compression and hence reduces the elastic energy required for attachment. The result is that the attachment rate is enhanced by stretching. As a consequence, the elasticity of the system also increases with tension, and we find that the Nyquist plot exhibits a negative-viscosity loop, which grows steadily under tension. Thus the stretch-activated ATPase is accompanied by an increasing ability to perform oscillatory work, just as in real fibrillar flight muscle.

The response of the system to a sudden stretch demonstrates another aspect of stretch activation in the form of the delayed rise in tension after the initial rapid tension transient. The cross-bridge tilting rate quickly comes into balance with the enhanced attachment rate at the start of the cross-bridge cycle, whereas the dissociation rate at the end of the cycle only builds up slowly. The result of the interplay between these different processes is a slow rise in the occupation probability  $p_{345}$  after the power stroke and a corresponding slow rise in the delayed tension. The same balance of factors underlies the negative-viscosity loop. Hence we have shown that stretch activation may be a natural consequence of quite simple cross-bridge kinetics.

### APPENDIX I: STEADY-STATE PROBABILITIES

At steady state, the time derivatives in the rate equations, Eqs. 6a–e, are zero, and we are left with five simultaneous equations that determine the steady-state occupation probabilities. Their solution is particularly straightforward if we make the simplifying approximation  $k_{05} = 0$ , and it may be written in the form

$$p_5/p_4 = k_{45}/(k_{50} + k_{54}), \quad (13a)$$

$$p_4/p_3 = k_{34}/(k_{43} + k_{45} - k_{54}p_5/p_4), \quad (13b)$$

$$p_3/p_2 = k_{23}(x)/(k_{32} + k_{34} - k_{43}p_4/p_3), \quad (13c)$$

$$p_2/p_1 = k_{12}/(k_{23}(x) + k_{21} - k_{32}p_3/p_2), \quad (13d)$$

$$p_1/p_0 = k_{01}(x)/(k_{10} + k_{12} - k_{21}p_2/p_1), \quad (13e)$$

where

$$p_0 = \frac{1}{1 + p_1/p_0(1 + p_2/p_1(1 + p_3/p_2(1 + p_4/p_3(1 + p_5/p_4))))} \quad (14)$$

## APPENDIX II: THE COMPLEX ELASTIC CONSTANT

We present here an outline of the mathematics required to derive an expression for the frequency-dependent complex elastic constant  $\lambda(\omega)$  of a cross-bridge, as defined in Eq. 11. Introducing an oscillatory displacement of amplitude  $\delta x$  as in Eq. 8, we find that Eqs. 6a–e become

$$(j\omega + 1/\tau_1)\delta p_1 + (k_{01}(x) - k_{21})\delta p_2 \quad (15a)$$

$$+ k_{01}(x)(\delta p_3 + \delta p_4 + \delta p_5) = A \delta x,$$

$$-k_{12}\delta p_1 + (j\omega + 1/\tau_2)\delta p_2 - k_{32}\delta p_3 = B \delta x, \quad (15b)$$

$$-k_{23}(x)\delta p_2 + (j\omega + 1/\tau_3)\delta p_3 - k_{43}\delta p_4 \quad (15c)$$

$$= -B \delta x,$$

$$-k_{34}\delta p_3 + (j\omega + 1/\tau_4)\delta p_4 - k_{54}\delta p_5 = 0, \quad (15d)$$

$$-k_{45}\delta p_4 + (j\omega + 1/\tau_5)\delta p_5 = 0, \quad (15e)$$

where  $1/\tau_1 = k_{01}(x) + k_{10} + k_{12}$ ,  $1/\tau_2 = k_{21} + k_{23}(x)$ ,  $1/\tau_3 = k_{32} + k_{34}$ ,  $1/\tau_4 = k_{43} + k_{45}$ ,  $1/\tau_5 = k_{50} + k_{54}$ ,  $A = p_0 dk_{01}(x)/dx$ , and  $B = -p_2 dk_{23}(x)/dx$ . The solution of the simultaneous Eqs. 15a–e is of the form

$$\delta p_i = E_i \delta p_1 + F_i \delta x, \quad (16)$$

for  $i = 2$  to  $4$ . The coefficients in this equation are found to be  $E_2 = k_{12}/D_{21}$ ,  $E_3 = k_{23}(x)E_2/D_{32}$ ,  $E_4 = k_{34}E_3/D_{43}$ ,  $E_5 = k_{45}E_4/D_{54}$ ,  $F_2 = (1 - k_{32}/D_{32})B/D_{21}$ ,  $F_3 = (k_{23}(x)F_2 - B)/D_{32}$ ,  $F_4 = k_{34}F_3/D_{43}$ , and  $F_5 = k_{45}F_4/D_{54}$ , where  $D_{54} = j\omega + 1/\tau_5$ ,  $D_{43} = (j\omega + 1/\tau_4) - k_{54}k_{45}/D_{54}$ ,  $D_{32} = (j\omega + 1/\tau_3) - k_{43}k_{34}/D_{43}$ , and  $D_{21} = (j\omega + 1/\tau_2) - k_{32}k_{23}(x)/D_{32}$ .

The amplitude of the oscillatory component  $\delta p_1$  in the occupation probability  $p_1$  is therefore given by

$$\delta p_1 = \frac{A - (k_{01}(x) - k_{21})F_2 - k_{01}(x)(F_3 + F_4 + F_5)}{(j\omega + 1/\tau_1) + (k_{01}(x) - k_{21})E_2 + k_{01}(x)(E_3 + E_4 + E_5)} \delta x. \quad (17)$$

Substituting this into Eq. 16 for the other oscillatory components determines all of the terms on the right-hand side of Eq. 10. Hence the elastic constant  $\lambda(\omega)$  in Eq. 10 is also determined. It is straightforward to separate the above expressions into real and imaginary parts for evaluation on a computer. A copy of the Fortran program used to calculate the Nyquist plots in Fig. 4 may be obtained on request from the authors.

We are grateful to Dr. Mark Schoenberg for his helpful comments and encouragement during the preparation of this paper.

## REFERENCES

Abbott, R. H., and P. E. Cage. 1978. Periodicity in insect flight muscle stretch activation. *J. Physiol. (Lond.)* 289:32P.

- Campbell, K. S., and M. Lakie. 1996. Can the short range elastic component and thixotropy both be due to cross-bridge activity in relaxed muscle? *J. Physiol. (Lond.)*. In press.
- Chen, Y., and B. Brenner. 1993. On the regeneration of the actin-myosin power stroke in contracting muscle. *Proc. Natl. Acad. Sci. USA* 90: 5148–5152.
- Cooke, R. 1993. The structure of a molecular motor. *Curr. Biol.* 3:590–592.
- Curtin, N. A., and R. E. Davies. 1973. Chemical and mechanical changes during stretching of activated frog skeletal muscle. *Cold Spring Harb. Symp. Quant. Biol.* 37:619–626.
- Dantzig, J. A., Y. E. Goldman, N. C. Millar, J. Lactis, and E. Homsher. 1992. Reversal of the cross-bridge force-generation transition by photogeneration of phosphate in rabbit psoas muscle fibres. *J. Physiol. (Lond.)* 451:246–278.
- Deschevereskii, V. I. 1971. A kinetic theory of striated muscle contraction. *Biorheology*. 7:147–170.
- Finer, J. T., R. M. Simmons, and J. A. Spudich. 1994. Single myosin molecule mechanics: piconewton forces and nanometre steps. *Nature*. 368:113–119.
- Flitney, F. W., and D. A. Jones. 1990. Force production during stretch of active, fatigued, isolated mouse soleus muscles. *J. Physiol. (Lond.)* 424:55P.
- Herzig, J. W. 1977. A model of stretch activation based on stiffness measurements in glycerol extracted insect fibrillar flight muscle. *In Insect Flight Muscle*. R. T. Tregear, editor. North-Holland, Amsterdam. 209–219.
- Higuchi, H., T. Yanagida, and Y. E. Goldman. 1995. Compliance of thin filaments in skinned fibres of rabbit skeletal muscle. *Biophys. J.* 69: 1000–1010.
- Horiuti, K., K. Kagawa, and K. Yamada. 1994. The initial contraction of skinned muscle fibers on photorelease of ATP in the presence of ADP. *Jpn. J. Physiol.* 44:675–691.
- Huxley, A. F. 1957. Muscle structure and theories of contraction. *Prog. Biophys. Biophys. Chem* 7:255–318.
- Huxley, A. F. 1980. Reflections on Muscle. Liverpool University Press, Liverpool. 94.
- Huxley, A. F., and R. M. Simmons. 1971. Proposed mechanism of force generation in striated muscle. *Nature*. 233:533–538.
- Huxley, H. E. 1969. The mechanism of muscle contraction. *Science*. 164:1356–1366.
- Huxley, H. E., A. Stewart, H. Sosa, and T. Irving. 1994. X-ray diffraction measurements of the extensibility of actin and myosin filaments in contracting muscle. *Biophys. J.* 67:2411–2421.
- Ishijima, A., Y. Harada, H. Kojime, T. Funatsu, H. Higuchi, and T. Yanagida. 1994. Single-molecule analysis of the actomyosin motor using nano-manipulation. *Biochem. Biophys. Res. Commun.* 199: 1057–1063.
- Jewell, B. R., and J. C. Rüegg. 1966. Oscillatory contraction of insect fibrillar muscle after glycerol extraction. *Proc. R. Soc. Lond. B.* 164: 428–459.
- Julian, F. 1969. Activation in a skeletal muscle contraction model with a modification for insect flight muscle. *Biophys. J.* 9:547–570.
- Kawai, M., and P. W. Brandt. 1980. Sinusoidal analysis: a high resolution method for correlating biochemical reactions with physiological processes in activated skeletal muscles of rabbit, frog and crayfish. *J. Muscle Res. Cell Motil.* 1:279–303.
- Luo, Y., R. Cooke, and E. Pate. 1993. A model of stress relaxation in cross-bridge systems: effect of a series elastic element. *Am. J. Physiol.* 265:279–288.
- Machin, K. E., and J. W. S. Pringle. 1959. The physiology of insect fibrillar muscle. II. The mechanical properties of a beetle flight muscle. *Proc. R. Soc. Lond. B.* 151:204–225.
- Molloy, J. E., J. E. Burns, J. C. Sparrow, R. T. Tregear, J. Kendrick-Jones, and D. C. S. White. 1995. Single molecule mechanics of HMM and S1 interacting with rabbit or *Drosophila* actins using optical tweezers. *Biophys. J.* 68:298–305.
- Murase, M., H. Tanaka, K. Nishiyama, and H. Shimizu. 1986. A three-state model for oscillation in muscle: sinusoidal analysis. *J. Muscle Res. Cell Motil.* 7:2–10.

- Nishizaka, T., H. Miyata., H. Yoshikawa, S. Ishiwata, and K. Kinoshita. 1995. Unbinding force of a single motor molecule measured using optical tweezers. *Nature*. 377:251–254.
- Pringle, J. W. S. 1949. The excitation and contraction of the flight muscles of insects. *J. Physiol. (Lond.)*. 108:226–232.
- Rayment, I., H. M. Holden, M. Whittaker, C. B. Yohn, M. Lorenz, K. C. Holmes, and R. A. Milligan. 1993. Structure of the actin-myosin complex and its implications for muscle contraction. *Science*. 261:58–65.
- Reif, F. 1965. Chapter 15. In *Fundamentals of Statistical and Thermal Physics*. McGraw-Hill, New York.
- Rüegg, J. C., and H. Stumpf. 1969. Activation of the myofibrillar ATPase activity by extension of glycerol-extracted insect fibrillar muscle. *Pflügers Arch.* 305:34–46.
- Rüegg, J. C., and R. T. Tregear. 1966. Mechanical factors affecting the ATPase activity of glycerol-extracted insect fibrillar flight muscle. *Proc. R. Soc. Lond. B.* 165:497–512.
- Schoenberg, M., B. Brenner, J. M. Chalovich, L. E. Greene, and E. Eisenberg. 1984. Cross-bridge attachment in relaxed muscle. *Adv. Exp. Med. Biol.* 170:269–279.
- Schoenberg, M., and E. Eisenberg. 1985. Muscle cross-bridge kinetics in rigor and in the presence of ATP analogues. *Biophys. J.* 48:863–871.
- Slawnych, M. P., C. Y. Seow, A. F. Huxley, and L. E. Ford. 1994. A program for developing a comprehensive mathematical description of the crossbridge cycle of muscle. *Biophys. J.* 67:1669–1677.
- Squire, J. M. 1992. Muscle filament lattices and stretch-activation: the match-mismatch model reassessed. *J. Muscle Res. Cell. Motil.* 13: 183–189.
- Steiger, G. J. 1977. Stretch activation and tension transients in cardiac, skeletal and insect flight muscle. In *Insect Flight Muscle*. R. T. Tregear, editor. North-Holland, Amsterdam. 221–268.
- Thirlwell, H., J. E. T. Corrie, G. P. Reid, D. R. Trentham, and M. A. Ferenczi. 1994. Kinetics of relaxation from rigor of permeabilized fast-twitch fibers from rabbit using a novel caged ATP and apyrase. *Biophys. J.* 67:2436–2447.
- Thomas, N., and R. A. Thornhill. 1994a. Stretch activation of cross-bridges in fibrillar insect flight muscle. *J. Physiol. (Lond.)*. 480.P:76P.
- Thomas, N., and R. A. Thornhill. 1994b. Simulation of cross-bridge noise in fibrillar insect flight muscle. *J. Physiol. (Lond.)*. 480.P:77P.
- Thomas, N., and R. A. Thornhill. 1995a. Negative viscosity and non-linear elasticity of muscle cross-bridges. *Chaos Solit. Fract.* 5:393–406.
- Thomas, N., and R. A. Thornhill. 1995b. A theory of tension fluctuations due to muscle cross-bridges. *Proc. R. Soc. Lond. B.* 259:235–242.
- Thomas, N., and R. A. Thornhill. 1995c. Simulation of the effect of ADP on the response of rigorized cross-bridges to the release of caged ATP. *J. Physiol. (Lond.)*. 487.P:156P.
- Thomas, N., and R. A. Thornhill. 1995d. Monte Carlo simulation of cross-bridge noise in actomyosin. *J. Physiol. (Lond.)*. 487.P:156P–157P.
- Thomas, N., and R. A. Thornhill. 1995e. Relaxation of tension in fibrillar insect flight muscle. *J. Physiol. (Lond.)*. 483.P:195P–196P.
- Thomas, N., and R. A. Thornhill. 1996. Possible origin of tension oscillations in muscle preparations. *J. Physiol. (Lond.)*. In press.
- Thomas, N., R. A. Thornhill, and D. W. Keddie. 1993. Mechanical hysteresis and creep in rabbit psoas muscle fibres. *J. Physiol. (Lond.)*. 473:81P.
- Thornhill, R. A., and N. Thomas. 1993. Elasticity, hysteresis and noise for a two-state model of muscle cross-bridges. *J. Physiol. (Lond.)*. 467: 373P.
- Thorson, J., and D. C. S. White. 1969. Distributed representations for actin-myosin interaction in the oscillatory contraction of muscle. *Biophys. J.* 9:360–390.
- Thorson, J., and D. C. S. White. 1983. Role of cross-bridge distortion in the small-signal mechanical dynamics of insect and rabbit striated muscle. *J. Physiol. (Lond.)*. 343:59–84.
- Wakabayashi, K., Y. Sugimoto, H. Tanaka, Y. Ueno, Y. Takezawa, and Y. Amamiya. 1994. X-ray diffraction evidence for the extensibility of actin and myosin filaments during muscle contraction. *Biophys. J.* 67: 2422–2435.
- White, D. C. S., M. M. K. Donaldson, G. E. Pearce, and M. G. A. Wilson. 1977. The resting elasticity of insect fibrillar flight muscle and properties of the cross-bridge cycle. In *Insect Flight Muscle*. R. T. Tregear, editor. North-Holland, Amsterdam. 197–208.
- White, D. C. S., and J. Thorson. 1972. Phosphate starvation and the nonlinear dynamics of insect fibrillar flight muscle. *J. Gen. Physiol.* 60:307–336.
- White, D. C. S., and J. Thorson. 1975. *The Kinetics of Muscle Contraction*. Pergamon, Oxford.
- Wray, J. S. 1979. Filament geometry and the activation of insect flight muscle. *Nature*. 280:325–326.